# Interpretation of Thunderstorm Charging by the Polarization-Induction Mechanism

STIRLING A. COLGATE

*New Mexico Institute of Mining and Technology, Socorro 87801 and Los Alamos Scientific Laboratory*[1]
*University of California, Los Alamos, N. M. 87545*

ZEV LEVIN[2]

*National Center for Atmospheric Research,*[3] *Boulder, Colo. 80307*

ALBERT G. PETSCHEK

*New Mexico Institute of Mining and Technology, Socorro 87801*

(Manuscript received 25 January 1977, in revised form 6 June 1977)

ABSTRACT

The numerical calculations of the combined stochastic growth and induction charging due to drop interactions by Scott and Levin (1975) are analyzed in terms of a phenomenological model. The assumed initial drop size distribution which is concentrated around 20 $\mu$m radius evolves at one point in time to a two-peaked distribution at 20 and 150–200 $\mu$m, respectively. We show that when this two-peaked distribution occurs, the charging by the polarization-induction mechanism is powerful enough to overcome the several charge reduction mechanisms and to make the actual charge a significant fraction ($>\frac{1}{3}$) of the saturated charge for a wide range of parameters. The saturation charge is defined as the charge carried on the particle so that no charge will be separated on the average in subsequent interactions as long as the field remains the same. Also, using the actual charge, one predicts in agreement with the numerical calculations what range of parameters permits a full 7–8 $e$-folds ($e^7$–$e^8$) of electric field growth to take place before the small droplets are depleted.

## 1. Introduction

Detailed numerical calculations of the growth of electric fields in thunderstorms based on the mechanism of polarization-inductive charging by drop scattering in an electric field have been made in a series of papers (Scott and Levin, 1974, 1975). These numerical analyses supplement the initial theoretical concepts of Sartor (1967), Mason (1972) and Paluch and Sartor (1973). We attempt here to reproduce the numerical calculations with an analytic calculation. Our emphasis is to understand the stochastic calculations and not necessarily to settle questions of the true nature of thunderstorm charging. We make it possible to calculate the charging rate without recourse to a computer. This is important because the characteristics of the collisions are not well known and are disputed. Workers without access to computers should be able, by putting their parameters into our calculation, to calculate charging rates and rates of field growth. Experimenters should be able to ascertain the parameters whose measurement will most effectively improve predictions.

We will consider the growth of the field only as long as the effects of the electrical forces on the fall velocities of the particles can be neglected. This means that the present calculations will be relevant for fields which are about $e^7$ times (7 generations above) the fair weather field. The effect of the electrical forces when the electric field is higher must be examined separately. One of the points we should like to investigate concerns the comparison of the electric field growth rate and the growth of drops by collection. This exact point was numerically modeled in a stochastic mode by Scott and Levin (1975), but our purpose is to elucidate wherever possible the critical parameters used in the modeling.

Moore (1975a) has questioned the charge separation limit due to the bouncing of drops at large angles of interaction. In addition, Moore (1974) and Colgate (1975) suggested that coalescence of particles may reduce the charging and the field growth, in effect short-circuit the charge generation mechanism. Levin and Scott (1975), on the other hand, pointed out that the numerical model of Scott and Levin did include all these hindering effects, but the charge generation

[1] LASL is operated under the auspices of USERDA.

[2] On sabbatical leave (1976–77) from the Department of Geophysics and Planetary Sciences, Tel Aviv University, Ramat Aviv, Israel, where part of this work was carried out.

[3] The National Center for Atmospheric Research is sponsored by the National Science Foundation.

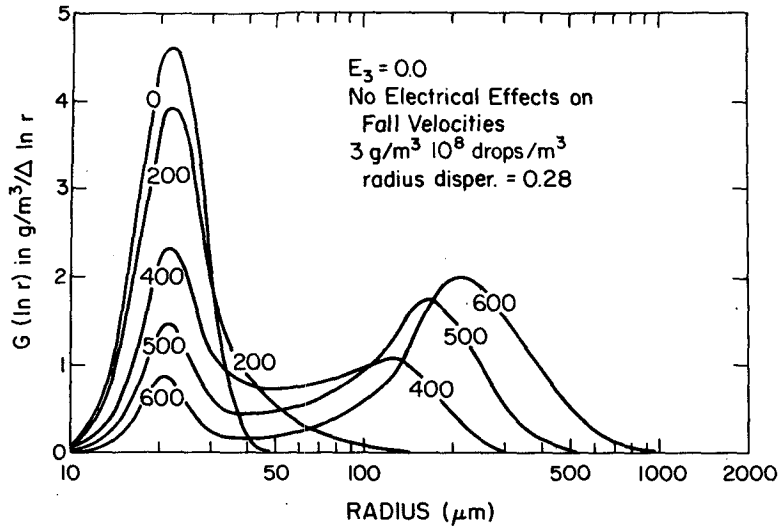


FIG. 1. The evolution of the liquid water content per logarithmic radius interval versus logarithm of drop size for $E_3=0.0$ from Levin (1976). The numbers on the curves represent time in seconds.

mechanism was powerful enough to overcome them and to produce strong fields. In this paper we compare approximately and analytically the growth rates of the particles by collection with the rates of charge separation and charge neutralization. These will be compared as a function of two parameters: $E_2$, the coalescence efficiency (defined as the probability that two particles will merge if one overtakes the other with an impact parameter less than the sum of the radii) and $E_3$, the contact efficiency (the probability that two particles have made electrical contact although they failed to merge). The probability that the particles neither merge nor make electrical contact is then $(1-E_2)(1-E_3)$.

In the polarization-induction charging mechanism charge is separated during each collision with electric contact in proportion to the ambient electric field and to the charges carried by the particles prior to the interaction. For small initial charges, charge can be separated in such a way that, for example, the large particle will gain negative charge and the small one positive charge. However, if the initial charge is just right ("saturated") the net charge transfer could be zero.

We find a relatively simple condition based on saturated charging which determines whether the field can grow to a value $e^{7.5}$–$e^8$ times its initial value. The proximity of the actual charge on the large drop to the saturated charge is controlled by competition between the drop growth (by collection of neutral or oppositely charged particles) and the growth of the drop charge. Here we would like to determine the limits of the parameters for which collision charging dominates and compare these with the results of the numerical model.

## 2. Drop growth by collection

The cloud drop size distribution evolves primarily by collection of smaller drops on larger ones. This process proceeds rapidly once a few large drops (e.g., $r \gtrsim 20$ μm) exist among all the smaller drops formed by condensation. In fact, condensation continues to modify the drop size distribution even later when the drops are larger (Kovetz and Olund, 1969), but this process is neglected here.

If the drop size distribution rapidly develops into a bimodal distribution in which the liquid water content is equally divided between the first mode around $\langle r_n \rangle = 20$ μm and the second at $\langle r_m \rangle = 150$ μm, then a continuous rather than stochastic approach might be justified. Once this bimodal distribution is formed, the liquid water content of the first peak, $\rho_{Ln}$, is progressively depleted and the peak around $r_m$ monotonically moves up to larger radii. These distributions are shown in Fig. 1 (from Levin, 1976).

The interactions of the particles and the field growth depend on the fall velocities of the particles and it is important for our treatment here to find a simple expression for these velocities. Since we are not concerned with the effects of the electrical forces on the fallspeeds of the particles, we can take the results of fall velocities in the unelectrified case from Scott and Levin as depicted in Fig. 2. As we know, the complexities of this curve are due to the transition from laminar to turbulent flow. In the laminar region, $V \propto r^2$ corresponding to the $r^2$ line that fits the curve for $r<60$ μm. Above this point we have decomposed the curve into a region where $V \propto r$ and $V \propto r^{\frac{1}{2}}$. The last region occurs due to a constant drag coefficient when the Reynolds number $\gtrsim 100$ and $r>600$ μm. The

corresponding velocity functions are as follows:

$$\left.\begin{aligned}
&\text{I. } V=V_{\mathrm{I}}r^2\ [\mathrm{m\ s^{-1}}];\\
&\qquad V_{\mathrm{I}}=1.3\times10^{8}\ \mathrm{m^{-1}\ s^{-1}},\quad r\leqslant 61.5\ \mu\mathrm{m}\\
&\text{II. } V=V_{\mathrm{II}}r\ [\mathrm{m\ s^{-1}}];\\
&\qquad V_{\mathrm{II}}=8\times10^{3}\ \mathrm{s^{-1}},\quad 61.5\leqslant r\leqslant 625\ \mu\mathrm{m}\\
&\text{III. } V=V_{\mathrm{III}}r^{\frac{1}{2}}\ [\mathrm{m\ s^{-1}}];\\
&\qquad V_{\mathrm{III}}=2\times10^{2}\ \mathrm{m^{\frac{1}{2}}\ s^{-1}},\quad 625\leqslant r\ \mu\mathrm{m}
\end{aligned}\right\},\quad (1)$$

where $r$ is in meters. The initial coalescence occurs within region I. However, we are interested in comparing the particle growth with the field growth during the time in which the field growth rate is maximum. This occurs between 400–600 s when the electric field grows by 5–7 $e$-folds according to the numerical calculations and where we believe that simplified analytical arguments may be applied.

Fig. 1 indicates that the general trend during this time is the formation of a peak around 150 $\mu$m radius, with a reduction of the peak around 20 $\mu$m radius.

At this stage, it is worth calculating the rate at which the drops around 150 $\mu$m grow by accreting smaller drops. We assume that the growth of 150 $\mu$m radius drops (when the liquid water content is about equal under each peak in Fig. 1) is due to the accretion of 20 $\mu$m drops and not due to collisions between the larger drops themselves. To the extent that this may be true, accretion of the smaller drops $r_n$ by the larger ones $r_m$ represents an incremental increase in volume of the larger drops. The growth rate can be expressed in terms of a characteristic growth time

$$\tau_g=\left(\frac{1}{r_m}\frac{dr_m}{dt}\right)^{-1}=3\left(\frac{1}{\mathrm{Vol}}\frac{d\,\mathrm{Vol}}{dt}\right)^{-1}$$

$$=\frac{3r_m^3}{r_n^3 n_n \pi V (r_n+r_m)^2 E_2},\quad (2)$$

where $V$ is the velocity difference.

Since, as Moore (1975b) has pointed out, updraft velocities are seldom large enough to replenish the condensation droplets, the growth of the larger droplets must be at the expense of the smaller ones. If $\rho_{Lm}=\rho_{Ln}$ the small droplets must all be swept out in the time required for the large drops to double in volume. To obtain large fields we must then have a characteristic growth time for the field which is several (7 or 8) times smaller than $\tau_g$. If we use, following Whelpdale and List (1971), $E_2=(1+r_n/r_m)^{-2}$ and neglect the fallspeed of the small droplets, then Eq. (2) simplified to $\tau_g=4/V_{\mathrm{II}}\rho_{Ln}$ or $5\times10^{-4}/\rho_{Ln}$ seconds if $\rho_{Ln}$ is the (dimensionless) fraction of cloud volume occupied by small droplets, about $1.5\times10^{-6}$ in Scott and Levin. This agrees with the evolution time implied by Fig. 1. With this qualitative understanding of the drop size evolution rate, we turn to its effects upon collisional induction charging.

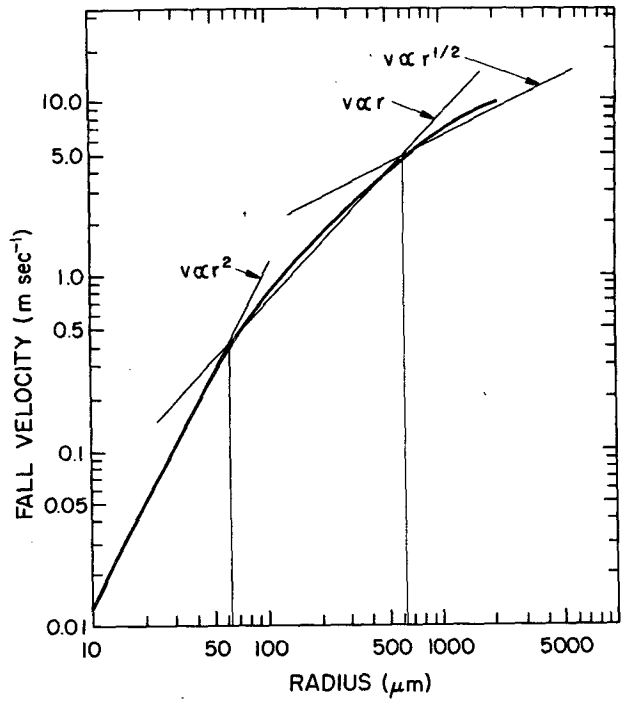


FIG. 2. Terminal fall velocities of drops as a function of radius. The straight lines are drawn to approximate the three regions of functional dependence described in Eq. (1).

## 3. The charge limit

The charge transfer in a collision without coalescence in which electrical contact is made can be obtained by setting the electrical field between the particles to zero in Davis' (1964)[4] calculation of the electric field between charged conductors. The increment of charge given to the larger particle of radius $r_m$ in an electric field $F$ by an interaction with a smaller particle in radius $r_n$ is

$$\Delta Q_{nm}=-4\pi\epsilon_0\phi F r_n^2\langle\cos\theta\rangle+(\omega-1)Q_m+\omega Q_n,\quad (3)$$

where $Q_n$ and $Q_m$ are the charges on the smaller and larger particle, respectively, prior to the interaction and $\theta$ is the angle between the electric field and the line connecting the drops' centers upon separation; $\epsilon_0$ is the permitivity of free space ($8.85\times10^{12}\ \mathrm{C^2\,n^{-1}\,m^{-2}}$). The electric field $F$ is taken to point toward negative charge, and $\phi$ and $\omega$ are geometrical factors which depend on the ratio of the sizes of the interacting particles. From the results of Ziv and Levin (1974), $\phi$ can be approximated by

$$\phi\approx1.6(r_m/r_n)^{\frac{1}{2}}\quad\text{for}\quad 1\leqslant r_m/r_n\leqslant 10.\quad (4)$$

Major, or significant, contributions to charge separation evidently do not fall outside this radius ratio

[4] Davis (1964) and Scott and Levin (1975) used electrostatic units (esu) in their calculations. Due to the AMS policy of using SI units, the present derivations are carried out in MKS units.

limit by a sufficient margin to invalidate the subsequent conclusions. An average over $\cos\theta$ must be performed subject to constraints of aerodynamics and charge-dependent contact or coalescence. If, for example, we choose a mean value of $\cos\theta=1/1.6$ ($\theta=51.3°$) and assume that both interacting particles are uncharged then $\Delta Q_{nm}=-4\pi\epsilon_0 F r_n^2$ for $r_n\approx r_m$. That is, two initially neutral drops separate charge such that the final electric field at their surface is equal to the ambient electric field

$$Q_n=-Q_m=-\Delta Q_{nm}=4\pi\epsilon_0 F r_n^2.$$

The last two terms in Eq. (3) (which include the charge on the particles prior to the interaction) represent a limitation to the actual charge that can be separated in each collision. Therefore, there are some charges on the interacting particles for which no charge is transferred ($\Delta Q_{nm}=0$). Physically this can occur when the field on the drops' surfaces due to the charges is just equal and opposite to the polarization effects of the ambient field near the drops. The terms which include $\omega$, therefore, represent a natural saturation of the possible accumulated charge separated on either drop. However, when this process is considered for a full size distribution, it is easily seen that a condition of no charge transfer ($\Delta Q_{nm}=0$) may occur for some interactions under a certain ambient electric field but will not occur for other interactions under the same field. These last interactions will cause the field to change and hence to allow charge separation even among those particles that could not separate charge before.

It we assume that the charge transferred in Eq. (3) is limited first by $Q_m$ and then by $Q_n$, then the saturation value on the larger particle is given by

$$0=\Delta Q_{nm}=-4\pi\epsilon_0\phi F r_n^2\langle\cos\theta\rangle+(\omega-1)Q_{m\,\mathrm{sat}}$$

or

$$|Q_{m\,\mathrm{sat}}|=\frac{4\pi\epsilon_0\phi F r_n^2\langle\cos\theta\rangle}{\omega-1}. \tag{5}$$

Our inspection of Table 1 of Ziv and Levin (1974) shows that $\phi r_n^2/(\omega-1)r_m^2=-3.1\pm0.05$ for $1\geqslant r_n/r_m\geqslant 0.1$ so that

$$|Q_{m\,\mathrm{sat}}|=4\pi\epsilon_0\,3.1F r_m^2\,\langle\cos\theta\rangle. \tag{6}$$

Similarly the small drop charge becomes saturated when the last term on the right hand side in Eq. (3) balances the induction terms. Using $\phi/\omega\approx 3.24(r_m/r_n)^{1/6}$ for $0.1\leqslant r_n/r_m\leqslant 1$, obtained again by inspection of the numerical table of Ziv and Levin (1974), gives

$$|Q_{n\,\mathrm{sat}}|=4\pi\epsilon_0 F r_n^2\frac{\phi}{\omega}\langle\cos\theta\rangle\approx 4\pi\epsilon_0 3.24F r_n^2\times\langle\cos\theta\rangle\left(\frac{r_m}{r_n}\right)^{1/6}. \tag{7}$$

Note that the saturation charge of each drop category is conveniently expressed primarily in terms of its own radius. While the actual saturation charges [Eqs. (6) and (7)] depend on $\cos\theta$, we shall be dealing only with average charges, and shall therefore only require $\langle\cos\theta\rangle$.

Using Eq. (4), Eq. (3) is conveniently rewritten in terms of the drop size ratio $p=r_n/r_m$ and the relative saturations, $q_m=Q_m/Q_{m\,\mathrm{sat}}$ and $q_n=Q_n/Q_{n\,\mathrm{sat}}$ as

$$\Delta Q_{nm}=-4\pi\epsilon_0 F r_n^2\,1.6p^{-\frac{1}{2}}(1-q_m-q_n). \tag{8}$$

Also, the following condition for cloud neutrality in terms of the relative saturations is obtained by equating the total charge on the large and small drops to zero, i.e.,

$$\frac{q_n}{q_m}=\frac{\rho_{Lm}}{\rho_{Ln}}\left(\frac{3.1}{3.24}\right)p^{7/6}. \tag{9}$$

The question we seek to answer is how close to saturation we can expect the drop charges to be and whether this is sufficient to generate the large rates of field growth observed in thunderstorms. Charge-separating collisions tend to bring about saturated charging. Deviations from saturated charging are brought about by coalescence which not only increases the size of the drop, making the saturated charge larger, but also tends to reduce the actual charge on the large drops because the small droplets are oppositely charged to them. Further deviations are caused by field growth, which increases the saturated charge without affecting the actual charge.

The competition among these processes is the subject of the following sections.

## 4. Coalescence with neutral small drops

The question posed in the last section can be visualized in Fig. 3 where we have plotted $Q/(-4\pi\epsilon_0 F r^2)$ vs log$r$ for a hypothetical large drop. Let us say that our drop starts at point A with radius $r_m$ and saturated charge $Q_{m\,\mathrm{sat}}\approx-4\pi\epsilon_0 F r^2$. By accretion growth it moves from $r_m$ to $r_m'=r_m(1+\delta)$ such that the saturated charge at $r_m'$ *would* be $Q_{m\,\mathrm{sat}}'=Q_{m\,\mathrm{sat}}(1+2\delta+\delta^2)\approx Q_{m\,\mathrm{sat}}(1+2\delta)$. Then the amount of charge to be added in order to maintain saturation becomes $Q=Q_{m\,\mathrm{sat}}'-Q_{m\,\mathrm{sat}}=2Q_{m\,\mathrm{sat}}\delta$. The mass of water to be added becomes to a first approximation

$$((M'-M)=3M\delta=4\pi r_m^3\delta. \tag{10}$$

If this water is added to the large drop by accretion of drops of mean radius $r_n$, then the number of collisions with coalescence efficiency $E_2$ which needs to occur becomes

$$N=\frac{M\delta}{E_2(4\pi/3)r_n^3}=\frac{3}{E_2}\left(\frac{r_m}{r_n}\right)^3\delta. \tag{11}$$

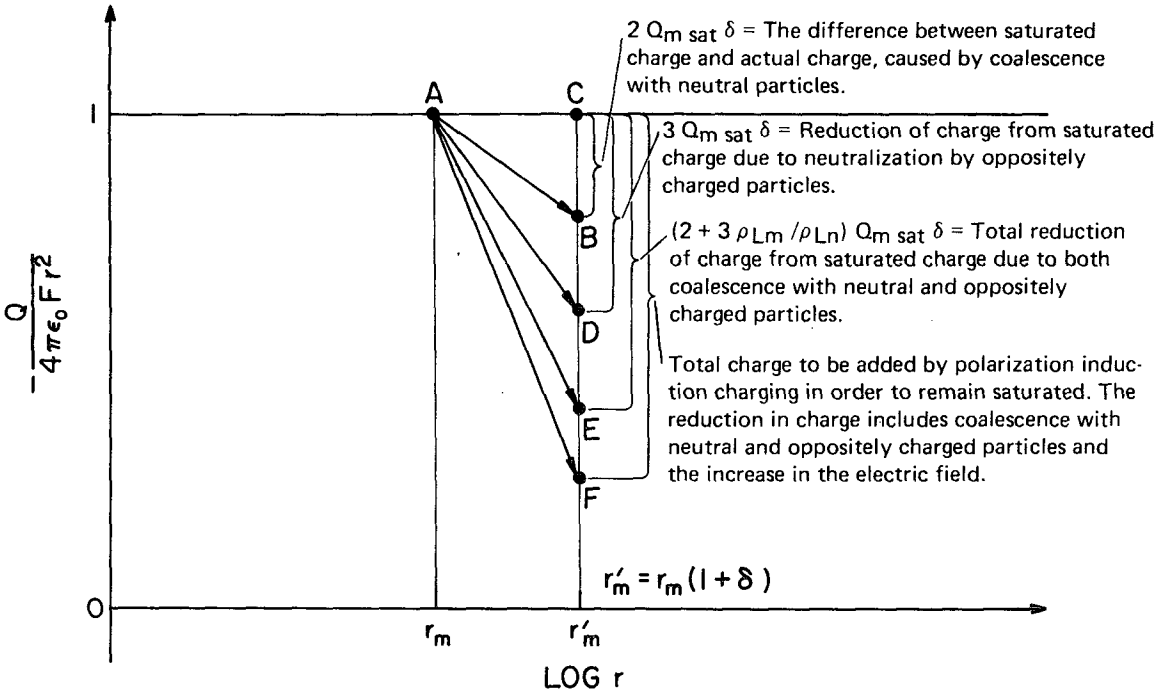


FIG. 3. Hypothetical variation of large drop charge with drop size. The ordinate is $Q/(-4\pi\epsilon_0 F r^2)$ and the saturation value is shown as a horizontal line. Point A is the starting point, Point B is the value of $Q/(-4\pi\epsilon_0 F r_m^2)$ when the radius has been increased from $r_m$ to $r_m(1+\delta)$, by coalescence with uncharged drops. Point C corresponds to saturated charging and the difference between B and C is the charge that has to be added to maintain the saturated condition. Point D corresponds to the charge due to neutralization following coalescence with smaller drops of equal and opposite charge per unit mass. Point E is the sum of the two effects. Point F corresponds to the change in the saturated charge on the drop due to the increase in the ambient field. Therefore, the total charge that has to be separated in order to remain saturated is the difference between points F and C.

If none of these coalescing drops either carried charge nor separated charge, then the large drop would move to point B in Fig. 3 where

$$\frac{Q}{r^2}=\frac{Q_{m\,\mathrm{sat}}}{(r_m')^2}=\frac{Q_{m\,\mathrm{sat}}}{r_m^2(1+2\delta)}. \tag{12}$$

This means that, in order for the large drop to remain saturated, the amount of charge that has to be separated by collisions with small drops is $\Delta Q=2Q_{m\,\mathrm{sat}}\delta$, and is shown as the difference between point B and the line $Q/(-4\pi\epsilon_0 F r^2)=1$ in Fig. 3.

The charging rate will be zero if the actual charge on the drops remains saturated at all times. Therefore, the charge on the drops will be a fraction $q_m$ of $Q_{m\,\mathrm{sat}}$, say $Q_m=q_m Q_{m\,\mathrm{sat}}$. Since $N$ is the number of collisions taking place in a unit time ($E_2N$ is the fraction of the collisions that actually coalesced), then for the large drop to remain charged with charge $Q_m$ the charging rate has to equal or exceed the rate at which charge becomes deficient due to coalescence, or

$$E_3(1-E_2)N\Delta Q_{nm}=2Q_m\delta. \tag{13}$$

## 5. Coalescence with oppositely charged small drops

If, as expected, the smaller drops have, on the average, opposite charge from the larger drops, then their coalescence with a larger drop will decrease the net charge of the large drop in addition to increasing its volume and hence will increase the charge necessary to maintain saturation. On the average the total positive charge on the smaller drops must equal the total negative charge on the larger drops by charge conservation (assuming no discharge to the atmosphere). Then the larger drops will coalesce with smaller drops whose charge per unit cloud volume is the same as the average of the larger ones but of opposite sign ($Q_n\rho_{Ln}/M_n=-Q_m\rho_{Lm}/M_m$, where $M_m$, $M_n$ are droplet masses). Therefore, if the larger drop increases its mass by $3M\delta$ in evolving from A and B, (see Fig. 3) it is likely to reduce its negative charge from A to D by an amount $3Q_{m\,\mathrm{sat}}(\rho_{Lm}/\rho_{Ln})\delta$. Without any charging the drop would therefore move to the point E in Fig. 3 where its charge is reduced by $(2+3\rho_{Lm}/\rho_{Ln})Q_{m\,\mathrm{sat}}\delta$. This is also the negative charge to be added by induction charging in order that the larger drop remain at saturation charge. However, as was pointed out before we do not expect the charge on the large drop to be at saturation since then no charge will be separated. Therefore, we are concerned with the negative charge to be added by induction charging to cover the reduction of charge from $Q_m=q_m Q_{m\,\mathrm{sat}}$, or $(2+3\rho_{Lm}/\rho_{Ln})Q_m\delta$.

### 6. The effect of the field growth on the saturated charge

One other process that increases the amount of charge needed to achieve saturation is the growth of the electric field during the time that the drops interact. This field growth is a result of charge separation by differential gravitational settling of drops that have undergone charge separation earlier. In other words, during the time that the drop grew by coalescence so that its charge was reduced to point E in Fig. 3, the field grew by some $\Delta F$ so that the new saturation charge is now higher and the polarization-induction charging has to be powerful enough to provide enough charge, as is shown schematically by the distance between point F and the line $-Q/(-4\pi\epsilon_0 F r^2)=1$ in Fig. 3.

To describe this analytically we first note that with the effect of coalescence and neutralization only the charge to be added (again with the use of $Q_m$ instead of $Q_{m\,\mathrm{sat}}$) could be written as

$$\Delta Q=(2+3\rho_{Lm}/\rho_{Ln})Q_m\delta=\frac{(2+3\rho_{Lm}/\rho_{Ln})}{r_m}\frac{dr_m}{dt}Q_m\Delta t. \quad (14)$$

Since the saturated charge is proportional to $F$, the fractional charge to be added to the drop due to the increase in the field from $F$ to $F+\Delta F$ is proportional to $\Delta F/F$. This implies that the total charge to be added due to coalescence, neutralization and field growth is

$$\Delta Q=\frac{(2+3\rho_{Lm}/\rho_{Ln})}{r_m}Q_m\frac{dr_m}{dt}\Delta t+\frac{Q_m}{F}\frac{dF}{dt}\Delta t \quad (15)$$

and the required charging rate is

$$\frac{dQ}{dt}=q_m Q_{m\,\mathrm{sat}}\left(\frac{(2+3\rho_{Lm}/\rho_{Ln})}{r_m}\frac{dr_m}{dt}+\frac{1}{F}\frac{dF}{dt}\right). \quad (16)$$

If the cloud were horizontally infinite and plane the field would grow at a rate $dF/dt=n_m V Q_m/\epsilon_0$ where $V$ is the relative fall velocity of the particles. We shall modify this expression by adding a geometrical factor $f$ by which finite cloud size effects and the confinement of the cloud between the ground and the ionosphere reduce the rate of field growth and a discharge current $J_D$ to obtain

$$\frac{dF}{dt}=(n_m V Q_m f-J_D)/\epsilon_0. \quad (17)$$

The first term in the parentheses is the generating current and the second term represents the discharge current due to ion conduction. In the numerical model $J_D$ was assumed to increase with the ambient electric field in a form close to that given by Mason (1972)[5], i.e.,

$$J_D=\tfrac{1}{3}\times 10^{-8}[\exp(6.7\times 10^{-6}F)-1]\ [\mathrm{A\ m^{-2}}]. \quad (18)$$

The value of the exponent at the maximum growth rate, $t=500$ s, is less than unity (see Fig. 4). We can therefore expand the exponential term in Eq. (18) and keep only the first order. Since $J_D$ tends to slow down the field growth we would like to determine its time constant,

$$\tau_D=\frac{F}{(dF/dt)_D}=\frac{\epsilon_0 F}{J_D}\approx 398\ \mathrm{s}. \quad (19)$$

We have not included in our model a discharge current between oppositely charged droplets since we are considering charges well below the threshold for corona or sparking. Discharge using the conductivity of cloudy air is known to be negligible (e.g., Scott and Levin, 1975; Rust and Moore, 1974). We can now write Eq. (17) as

$$\frac{1}{F}\frac{dF}{dt}=\frac{n_m V Q_m f}{\epsilon_0 F}-\tau_D^{-1}. \quad (20)$$

Combining Eq. (20) with (16) and obtaining the ratio of charging rate to growth rate from Eq. (8) and $\Delta r=r_n^3/3r_m^2$ we get after some algebra

$$1.55\left(\frac{1-E_2}{E_2}\right)E_3\left(\frac{r_m}{r_n}\right)^{\frac{1}{2}}(1-q_m-q_n)=q_m\left[(2+3\rho_{Lm}/\rho_{Ln})-\frac{\tau_D^{-1}r_m}{dr_m/dt}+\frac{3.1\times 4\pi r_m^3 n_m V\langle\cos\theta\rangle q_m f}{dr_m/dt}\right]. \quad (21)$$

By substituting $(1-E_2)/E_2=p(2+p)$ from Whelpdale and List's equation for $E_2$, $q_n=q_m(\rho_{Lm}/\rho_{Ln})\times(3.1/3.24)p^{7/6}$ from Eq. (9), $V=V_{\mathrm{II}}r_m$ from Eq. (1) and $dr_m/dt$ from Eq. (2), we obtain

$$1.55(2+p)p^{-\frac{1}{2}}\left[1-q_m\left(1+\frac{\rho_{Lm}}{\rho_{Ln}}\frac{3.1}{3.24}p^{7/6}\right)\right]E_3=q_m\left[(2+3\rho_{Lm}/\rho_{Ln})-\frac{4\tau_D^{-1}}{\rho_{Ln}V_{\mathrm{II}}}+\frac{\rho_{Lm}}{\rho_{Ln}}37.2\langle\cos\theta\rangle q_m f\right]. \quad (22)$$

hTis is a quadratic equation for $q_m$ from which we can deduce the behavior of the saturation charge. First of all, $p$ is small so the small drop saturation effect, the $p^{7/6}$ term, is negligible. Second, both the average collision angle $\langle\cos\theta\rangle$, which is poorly known, and the geometric factor $f$ appear only in the quadratic term. They will be important only if $q_m$ is appreciable. Of course, $\langle\cos\theta\rangle$ and $f$ enter more directly

[5] Here converted to MKS units.

into the field growth through the behavior of the saturated charge (see below).

For $\rho_{Ln}=\rho_{Lm}=1.5\times10^{-6}$ and $p=0.1$, Eq. (22) is reduced to

$$7.44f\langle\cos\theta\rangle q_m^2+[0.832+2.191E_3]q_m-2.057E_3=0. \quad (23)$$

Table 1 summarizes the values of $q_m$ from this equation as a function of $E_3$ and $f\langle\cos\theta\rangle$.

With this background we would like to compare the field growth rate with the drop growth rate by accretion and see whether the polarization-induction charging mechanism can maintain drop charges at sufficient level to lead to rapid field growth.

## 7. Field growth rate

By the use of Eq. (20) we can write

$$\tau_F^{-1}=\tau_C^{-1}-\tau_D^{-1}, \quad (24)$$

where

$$\tau_C^{-1}=\frac{n_m V Q_m f}{\epsilon_0 F}, \quad (25)$$

and where the charge separation current can be written

$$J=n_m V Q_m=n_m V Q_{m\,\mathrm{sat}} q_m$$
$$=\frac{4\pi\epsilon_0\rho_{Lm}\times3.1VFr_m^2\langle\cos\theta\rangle}{(4/3)\pi r_m^3}q_m. \quad (26)$$

This equation will have a maximum value when $V\propto r$ and when $\rho_{Lm}$ is concentrated in the 61–625 $\mu$m region of $V_{II}$ [Eq. (1)]. By neglecting $V_n$, the fall-speed of the smaller particles, so that $V=V_m-V_n\approx V_m$, we get

$$J=6.60\times10^{-7}F\rho_{Lm}\langle\cos\theta\rangle q_m\ [\mathrm{A\ m^{-2}}]. \quad (27)$$

By substitution into Eq. (25) we obtain

$$\tau_C=\frac{\epsilon_0 F}{Jf}=\frac{1.34\times10^{-5}}{\rho_{Lm}\langle\cos\theta\rangle f q_m}\ [\mathrm{seconds}]. \quad (28)$$

If $\rho_{Lm}=1.5\times10^{-6}$, $\langle\cos\theta\rangle=0.7$ and $f=1$, Eq. (28) becomes

$$\tau_C=\frac{12.8}{q_m}. \quad (29)$$

TABLE 1. Charge ratio $q_m=Q_m/Q_{m\,\mathrm{sat}}$ including the effects of coalescence, neutralization and field growth.

| $f\langle\cos\theta\rangle$ | $E_3$ = 1 | 0.8 | 0.5 | 0.3 | 0.1 | 0.05 |
|---|---|---|---|---|---|---|
| 1 | 0.361 | 0.328 | 0.264 | 0.205 | 0.110 | 0.070 |
| 0.7 | 0.402 | 0.366 | 0.296 | 0.230 | 0.122 | 0.077 |
| 0.3 | 0.498 | 0.457 | 0.373 | 0.289 | 0.149 | 0.090 |
| 0.1 | 0.594 | 0.550 | 0.454 | 0.352 | 0.174 | 0.101 |
| 0.05 | 0.631 | 0.587 | 0.488 | 0.379 | 0.184 | 0.105 |

TABLE 2. The time constant $\tau_F$ of the field growth and the total time $t_F$ available for field growth with time constant $\tau_f$ for $f=1$ and $\langle\cos\theta\rangle=0.7$.

| $E_3$ | 1.0 | 0.8 | 0.5 | 0.3 | 0.1 | 0.05 |
|---|---|---|---|---|---|---|
| $\tau_F$ | 34.6 | 38.3 | 48.5 | 64.7 | 142 | 285 |
| $t_F$ | 320 | 300 | 280 | 250 | 186 | 150 |
| $t_F/\tau_F$ | 9.1 | 7.9 | 5.7 | 3.9 | 1.3 | 0.5 |

By the use of Eq. (19) for $\tau_D$ and Eqs. (29) and (24), the time constant of the field growth becomes

$$\tau_F^{-1}=\frac{q_m}{12.8}-\frac{1}{398}. \quad (30)$$

By the use of Table 1 for $q_m$ as a function of $E_3$ we obtain the values of $\tau_F$ which are listed in Table 2.

## 8. Persistence of the charging mechanism

We now wish to improve our estimate of the time available for the charging mechanism to act from the crude value of $\tau_g$ in Eq. (2). From Eq. (28) we see that $\tau_c$ or $\tau_F$ depend on the product $\rho_{Lm}q_m$. Early in the coalescence process, the field growth is limited by the small value of $\rho_{Lm}$. Late in the process it will be cut off by a reduction in $q_m$. Then the charging process must change its nature, depending not on the condensation droplets but on the smaller of the coalesced drops that carry positive charge. We shall see that not many droplets are required to keep the charging process going, so that a few new condensation droplets formed in the updraft may also be significant.

To estimate the minimum small droplet concentration at which the charging mechanism persists, as we have described it, we write Eq. (22) in the form $aq_m^2+bq_m+c=0$, where only $c$ lacks a term of order $\rho_{Ln}^{-1}$. Hence for small $\rho_{Ln}$ the discriminant can be expanded in powers of $\rho_{Ln}$ and the solution $q_m$ will be of order $\rho_{Ln}$. This will cut off the field growth. The quadratic equation has a solution which is always smaller than both the small $c$ limit of $(-c/b)$ and the large $c$ limit of $(-c/a)^{\frac{1}{2}}$. Thus we may take the cutoff point at the intersection of these curves which, neglecting terms not of order $\rho_{Ln}^{-1}$ in $a$ and $b$ and the term containing $p^{7/6}$, is given by

$$\frac{\rho_{Ln}}{\rho_{Lm}}\approx\frac{\rho_{Ln}}{\rho_L}=\frac{(3-4/\tau_D V_{II}\rho_L)^2}{58f\langle\cos\theta\rangle(2+p)p^{-\frac{1}{2}}E_3}. \quad (31)$$

Since we assume here that the number of large drops does not change due to the lack of interaction between themselves, Eq. (2) can be regarded as an equation for $\rho_{Lm}$, namely

$$\frac{1}{\rho_{Lm}}\frac{d\rho_m}{dt}=\frac{3V_{II}\rho_{Ln}}{4}, \quad (32)$$

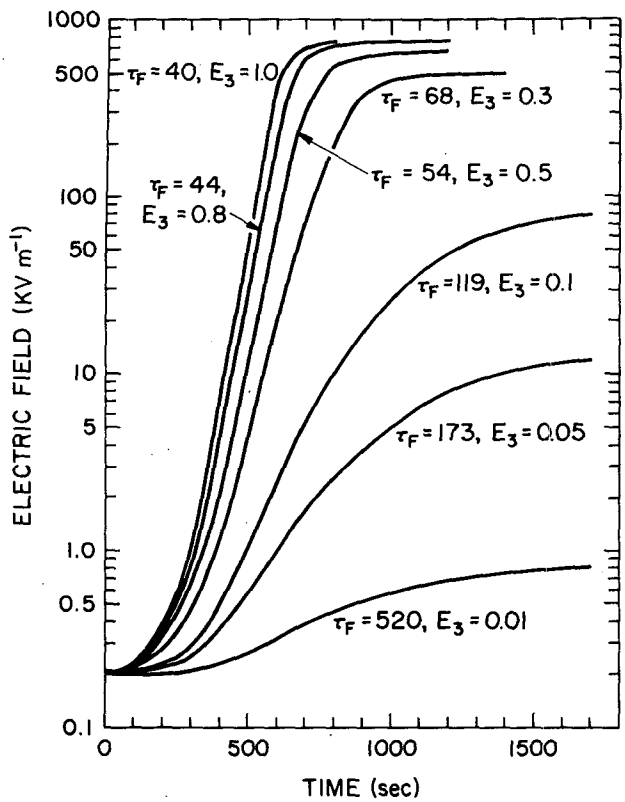


FIG. 4. The growth of the electric field as a function of time for various values of $E_3$ from Scott and Levin (1975). The values $\tau_F$ are the time constants corresponding to the maximum growth rate of the electric field at $t=500$ s. This is the time where the liquid water is about equally divided between the two peaks of the size distribution in Fig. 1.

which with the substitution $\rho_{Lm}=\rho_L-\rho_{Ln}$ can be integrated to give

$$t=-\frac{4}{3V_{\text{II}}\rho_L}\ln\frac{\rho_{Ln}}{\rho_L-\rho_{Ln}}, \tag{33}$$

where the origin of time has been chosen at $\rho_{Ln}=\rho_L/2$. When $\rho_{Ln}$ is smaller than the value given in Eq. (31), $q_m$ decays with the same time constant as $\rho_{Ln}$, namely $4/(3V_{\text{II}}\rho_L)$, giving an additional effective growth time of $4/(3V_{\text{II}}\rho_L)$. In addition, before the time in which $\rho_{Lm}=\rho_L/2$, $\rho_{Lm}$ has been growing with the same time constant. When these effective growth times are added to the times obtained by Eqs. (31) and (33) the total effective growth time becomes

$$t_F=\frac{4}{3V_{\text{II}}\rho_L}\left[2-\ln\left(\frac{(3-4/\tau_D V_{\text{II}}\rho_L)^2}{58f\langle\cos\theta\rangle(2+p)p^{-\frac{1}{2}}E_3}\right)\right]. \tag{34}$$

The values of $t_F$ obtained, given in Table 2, are larger than $\tau_g$. We observe from Table 2 that $t_F/\tau_F$ is $\gtrsim 8$ for $E_3>0.8$ and remains sufficient to account for several generations of field growth down to $E_3=0.3$ although here saturation is obtained by including the late charging mechanism produced by collisions among the larger droplets. This can be verified by reference to Figs. 4 and 5 which represent the field growth with time and the normalized current density as obtained from the numerical model. In Fig. 4 we see that the electric field reaches high values when $E_3=0.3$. Fig. 5 suggests that at later times (when $E_3=0.3$) the major portion of the positive charge is carried by

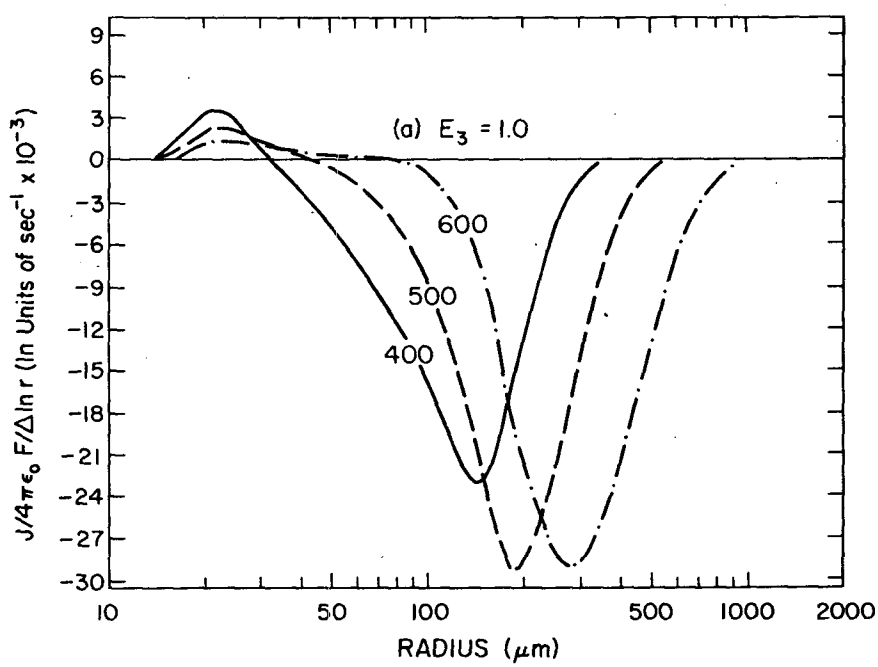

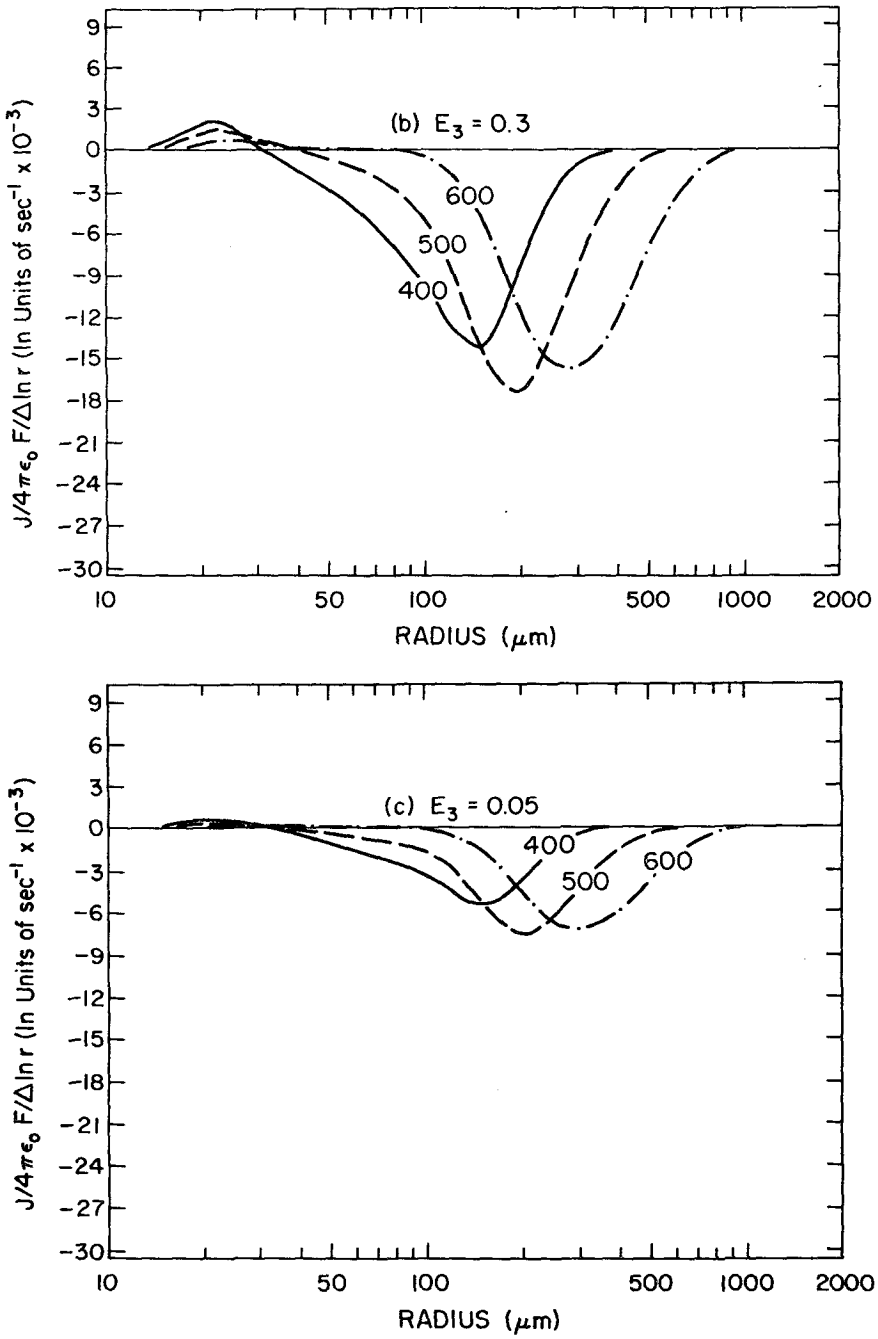


FIG. 5. The normalized current density per ($\Delta \ln r$) due to charge separation $[J/(4\pi\epsilon_0 F) = n\langle Q\rangle V/4\pi\epsilon_0 F$ per $\Delta \ln r]$ as a function of $\ln r$ for various times and values of $E_3$.

larger than 20 $\mu$m drops in agreement with the discussion above.

If low values of $\langle\cos\theta\rangle$ ($\sim$0.1) were chosen $t_F$ would be reduced by $4(\ln 0.7 - \ln\langle\cos\theta\rangle)/3V_{II}\rho_L) \sim 100$ s. Thus there would not be 8 generations of the field growth. This also agrees with Scott and Levin whose calculations dropped below 8 generations beginning with $\langle\cos\theta\rangle = 0.18$.

## 9. Comparison with the numerical calculations of Scott and Levin

Since the present calculations were carried out most precisely for the case when the liquid water is equally distributed between the small ($\sim$20 $\mu$m) and the large drops ($\sim$167 $\mu$m), the comparison with the numerical model is best undertaken for the field and charge development at $t \approx 500$ s. In Fig. 4 we plotted the

TABLE 3. Comparison between numerical calculations and theory [$\rho_L = 3\times10^{-6}$ ($m^3$ water/$m^3$ air) $t = 500$ s, $V_m = 1.67\times10^{-4}$ m $s^{-1}$].

| | | | Scott and Levin | | | | |
|---|---|---|---|---|---|---|---|
| $E_3$ | $F$ (V/m) [from Fig. 4] | $Q_{m\,sat}/F$ (C m $V^{-1}$) | $Q_m/F$ (C m $V^{-1}$) | $\frac{Q_m}{Q_{m\,sat}}$ | $\tau_F$ [from Fig. 4] (S) | $\frac{Q_m}{Q_{m\,sat}} = q_m$ [From Eq. (37)] | $\tau_F$ [From Table 4] (S) |
| 1.0 | $4.43\times10^4$ | $6.8\times10^{-18}$ | $2.176\times10^{-18}$ | 0.32 | 40 | 0.408 | 34.6 |
| 0.8 | $2.75\times10^4$ | $6.8\times10^{-18}$ | $1.97\times10^{-18}$ | 0.29 | 44 | 0.372 | 38.3 |
| 0.5 | $1.08\times10^4$ | $6.8\times10^{-18}$ | $1.63\times10^{-18}$ | 0.24 | 54 | 0.302 | 48.5 |
| 0.3 | $4.46\times10^3$ | $6.8\times10^{-18}$ | $1.29\times10^{-18}$ | 0.19 | 68 | 0.236 | 64.7 |
| 0.1 | $1.06\times10^3$ | $6.8\times10^{-18}$ | $7.48\times10^{-19}$ | 0.11 | 119 | 0.127 | 142 |
| 0.05 | $5.6\times10^2$ | $6.8\times10^{-18}$ | $5.03\times10^{-19}$ | 0.074 | 173 | 0.081 | 285 |

electric field growth curves from the calculations of Scott and Levin (1975) as a function of time and for various $E_3$. It can be seen that the maximum growth rate occurs at roughly the time when the water is equally divided between the two size peaks, namely around $t = 500$ s. The time constant for the field growth at $t = 500$ s is given on each curve.

When the values of $\tau_F$ from Fig. 4 are compared with those of Table 3 (for convenience $\tau_F$ from both Fig. 4 and Table 2 are also listed in Table 3), good agreement is obtained for large values of $E_3$ ($>0.3$).

Deviations at small $E_3$ probably occur because the numerical model used a slightly modified discharge current from that given by Eq. (18). Scott and Levin (1975) used

$$J_D = \tfrac{1}{3}\times10^{-8}[\exp(6.7\times10^{-6}F) - \exp(6.7\times10^{-6}F_0)], \quad (35)$$

where $F_0$ is the initial fair weather field. Scott and Levin used the second term in the brackets in order to make $J_D = 0$ at $t = 0$. When the value of $E_3$ is larger than about 0.3, this term has no effect on $\tau_F$ at 500 s, since $F/F_0 > 20$. But for smaller $E_3$ the field at 500 s is only slightly larger than $F_0$ and the contribution of the second term in the brackets of Eq. (32) to the value of $\tau_F$ is substantial.

Table 3 presents the values of $Q_m/F$ from the numerical computation at $t = 500$ s as a function of $E_3$. For comparison, $Q_{m\,sat}/F$ from Eq. (6) ($r_m = 167$ $\mu$m) and the electric field from the numerical model are given as well. Using these values the ratios $Q_m/Q_{m\,sat}$ in the numerical model have been computed. For comparison the values of $q_m$ from Table 1 for $\cos\theta = 0.7$ and $f = 1$ are also given. We see that $q_m$ in the numerical model is smaller than in the present calculation. These differences amount to only 9–25% at $E_3 = 0.05$ and $E_3 = 1.0$, respectively, and can be accounted for by the fact that in the numerical model drops of size $r_m$ interact both with smaller and larger drops. Interactions with larger drops transfer positive charge to $r_m$ while interactions with smaller drops transfer negative charge to it. These opposite charges that are transferred to $r_m$ result in smaller charges at $r_m = 167$ $\mu$m in comparison with the values calculated here.

In Fig. 5 we present the numerical results of the normalized current density per logarithmic radius interval resulting from the charge separated as a function of $\ln r$, time and $E_3$. We see that most of the current results from charge separation of particles of radii around 20 $\mu$m and 150–200 $\mu$m at times around 500 s which is precisely the time of the two peaked size distribution. This, of course, justifies the simplified assumptions made in this paper. We also see that the current density decreases with decreasing $E_3$ as expected.

In summary, we can say that our analysis confirms Scott and Levin's numerical calculation of saturated charging to a satisfactory degree.

It should be pointed out that the present calculations were carried out for cases where only water drops are present. In cases where ice is present similar calculations can be carried out with different values of the parameters $E_2$, $E_3$ and possibly $\langle\cos\theta\rangle$. It is believed that for ice particles interaction $E_2$ is considerably smaller and $\langle\cos\theta\rangle$ slightly larger. This would make the charge separation even more efficient than in the present calculations.

## 10. Conclusions

We have shown that the charge on the larger drops (when the two-peaked size distribution exists) is an appreciable fraction of the saturated charge, the saturated charge being defined as the charge on the particle so that no charge can, on the average, be separated by the induction charging in the ambient field. Only when the field changes or the size of the drop changes by coalescence can there be further induction charging. We have shown that the conditions for the charging mechanism to maintain a large fraction of saturated charge depends on the coalescence efficiency $E_2$. When the Whelpdale and List (1971) approximation to $E_2$ is used, the actual charge is a large fraction of the saturated charge when $E_3 > 0.3$ [see Scott and Levin (1975) or the text of this paper for the definitions of $E_3$]. This condition produces a field growth which

is 6–8 times faster than droplet growth by coalescence. Thus coalescence with small neutral and oppositely charged drops is not limiting the field growth as long as $E_3 \gtrsim 0.3$ in agreement with Scott and Levin (1975) and Levin and Scott (1975).

The results here and those of Scott and Levin (1975) depend on the angle of interaction ($\theta$) and on the values of $E_2$ and $E_3$ and their dependence on both $\theta$ and the ambient electric field. Not all these have been fully accounted for in either paper for lack of sufficient experimental data. This places a premium on a basic analytic understanding of the mechanism of field growth, which we hope we have supplied. We also hope to have pointed out which details of collision, charge separation and coalescence are important. On the other hand, the experimental observation of individual drop charge and size correlated with the local electric field will make a significant test of this mechanism in the electrical development of thunderstorms.

*Acknowledgments.* Stirling A. Colgate is indebted to C. B. Moore for encouragement and partial support under NSF Grant GI-33372X2 and GA-43933.

Zev Levin would like to thank W. D. Scott, J. Kuettner and J. D. Sartor for their review of the manuscript and I. Tzur for several constructive discussions.

Albert G. Petschek is supported in part by the Atmospheric Sciences Program of the National Science Foundation.

## REFERENCES

Colgate, S. A., 1975: Comment on "The electrification of thunderclouds and the rain gush." *J. Geophys. Res.*, **80**, 3913–3914.

Davis, M. H., 1964: Two charged spherical conductors in a uniform electric field: Forces and field strength. *Quart. J. Mech. Appl. Math.*, **17**, 499–511.

Kovetz, A., and B. Olund, 1969: The effect of coalescence and condensation on rain formation in a cloud of finite vertical extent. *J. Atmos. Sci.*, **26**, 1060–1065.

Levin, Z., 1976: A refined charge distribution in a stochastic electrical model of an infinite cloud. *J. Atmos. Sci.*, **33**, 1756–1762.

——, and W. D. Scott, 1975: Polarization charging may produce a large electric field before the radar echo maximum. *J. Geophys. Res.*, **80**, 3918–3923.

Mason, B. J., 1972: The physics of thunderstorms. *Proc. Roy. Soc. London*, **A327**, 433–466.

Moore, C. B., 1974: An assessment of thundercloud electrification mechanisms. *Proc. Int. Conf. Atmospheric Electricity*, Garmisch-Partenkirchen (in press).

——, 1975a: Rebound limits on charge separation by falling precipitation. *J. Geophys. Res.*, **80**, 2658–2662.

——, 1975b: Recombination limits on charge separation by hydrometeors in clouds. *J. Atmos. Sci.*, **32**, 608–612.

Paluch, I., and J. D. Sartor, 1973: Thunderstorm electrification by the inductive charging mechanism: I. Particle charges and electric fields. *J. Atmos. Sci.*, **30**, 1166–1173.

Rust, W. D., and C. B. Moore, 1974: Electrical conditions near the bases of thunderclouds over New Mexico. *Quart. J. Roy. Met. Soc.*, **100**, 450–468.

Sartor, J. D., 1967: The role of particle interactions in the distribution of electricity in thunderstorms. *J. Atmos. Sci.*, **24**, 601–615.

Scott, W. D., and Z. Levin, 1974: Stochastic rain development in an electrified cloud. *Preprints Conf. Cloud Physics*, Tucson, Amer. Meteor. Soc., 377–382.

——, and ——, 1975: A stochastic electrical model of an infinite cloud: Charge generation and precipitation development. *J. Atmos. Sci.*, **32**, 1814–1828.

Whelpdale, D. M., and R. List, 1971: The coalescence process in raindrop growth. *J. Geophys. Res.*, **76**, 2836–2856.

Ziv, A., and Z. Levin, 1974: Thundercloud electrification: Cloud growth and electrical development. *J. Atmos. Sci.*, **31**, 1652–1661.